



Acoustic Cluster Therapy (ACT) – pre-clinical proof of principle for local drug delivery and enhanced uptake



Annemieke van Wamel^{a,*}, Andrew Healey^b, Per Christian Sontum^b, Svein Kvåle^b, Nigel Bush^c, Jeff Bamber^c, Catharina de Lange Davies^a

^a Dept. of Physics, NTNU, Trondheim, Norway

^b Phoenix Solutions AS, Oslo, Norway

^c Joint Dept. of Physics, ICR, London, UK

ARTICLE INFO

Article history:

Received 16 November 2015

Received in revised form 11 January 2016

Accepted 12 January 2016

Available online 13 January 2016

Keywords:

Acoustic cluster therapy

ACT

Local drug delivery

PC-3 prostate adenocarcinoma

Pre-clinical

ABSTRACT

Proof of principle for local drug delivery with Acoustic Cluster Therapy (ACT) was demonstrated in a human prostate adenocarcinoma growing in athymic mice, using near infrared (NIR) dyes as model molecules. A dispersion of negatively charged microbubble/positively charged microdroplet clusters are injected i.v., activated within the target pathology by diagnostic ultrasound (US), undergo an ensuing liquid-to-gas phase shift and transiently deposit 20–30 μm large bubbles in the microvasculature, occluding blood flow for ~5–10 min. Further application of low frequency US induces biomechanical effects that increase the vascular permeability, leading to a locally enhanced extravasation of components from the vascular compartment (e.g., released or co-administered drugs). Results demonstrated deposition of activated bubbles in tumor vasculature. Following ACT treatment, a significant and tumor specific increase in the uptake of a co-administered macromolecular NIR dye was shown. In addition, ACT compound loaded with a lipophilic NIR dye to the microdroplet component was shown to facilitate local release and tumor specific uptake. Whereas the mechanisms behind the observed increased and tumor specific uptake are not fully elucidated, it is demonstrated that the ACT concept can be applied as a versatile technique for targeted drug delivery.

© 2016 Elsevier B.V. All rights reserved.

1. Introduction

Inadequate delivery into solid tumors is a well-recognized problem for a wide variety of drugs (e.g., chemotherapeutic agents), including small molecules, macromolecules such as monoclonal antibodies and cytokines, and nanoparticles with a variety of compositions. Once administered into the circulation, endothelial cells and other biological barriers restrict their passive extravasation into the tissue of the targeted pathology. Delivery of a systemically administered agent to cells within solid tumors involves three processes: distribution through the vascular compartment, transport across the microvascular wall or extravasation, and dispersion within the tumor interstitium [1]. However, for a number of drugs, the current, passive transvascular delivery paradigm is inefficient, and insufficient tumor penetration of therapeutic agents to reach effective local concentrations is often the outcome. In combination with low therapeutic indexes, increasing the dosages is not a viable strategy due to serious and wide spread adverse effects, overall limiting the clinical utility of a range of potent drugs.

Over the past decades, a range of strategies to overcome this fundamental problem and improve on the specificity of drug action has been explored. Active and passive approaches, exploiting particular cancer tumor characteristic such as design of drugs augmenting the Enhanced Permeability and Retention (EPR) effect, have been investigated extensively [2–5]. A range of drug carrier concepts, e.g., liposomes, micelles, dendrimers, nanoparticles have been employed, either to passively make use of the EPR effect or in combination with surface ligands that actively promote accumulation in tumor tissue through biochemically affinity to specifically expressed target groups. In many cases, these strategies have shown promise in pre-clinical studies, but transition to clinical practice with drugs designed to exploit the EPR effect has been very limited, with an exception for Doxil® [6] and possibly Abraxane® [7].

As an alternative approach, recent research and development have paid attention to externally activated drug delivery systems. Heat, light, ultrasound (US), electric and magnetic fields have been used as external energy sources for activating a drug formulation system in vivo for release and delivery of drugs at targeted locations within the body [8].

Over the past two decades, there has been growing interest in drug delivery using US, particularly in combination with regular contrast microbubbles such as Sonovue® or Optison® [9]. In brief, local US

* Corresponding author at: Institutt for fysikk, Norges teknisk-naturvitenskapelige universitet, 7491 Trondheim, Norway.

E-mail address: annemieke.wamel@ntnu.no (A. Wamel).

insonation of a pathologic condition (e.g., tumor) containing microbubbles in vascular compartments induces bubble oscillations (stable or inertial cavitation) which lead to a variety of biomechanical effects that enhance extravasation and distribution of drug molecules to target tissue [9–14]. This approach may hence be explored to improve on the local specificity of a drug, either co-injected with, or attached to microbubbles. Again, US in combination with microbubbles has shown promising results pre-clinically, but the approach has yet to reach regular clinical practice. Whereas the concept clearly holds merit, it also carries certain attributes that limits the effects. Used for local release, the microbubbles must be loaded with drug. In such a case, only a very thin stabilizing structure (e.g., phospholipid membrane or protein shell) is available for loading of microbubble formulations [15]. In addition, the circulation or lifetime of most microbubbles is typically on the order of 2–3 min, limiting the exposure time. Furthermore, the oscillating bubbles need to be close to the endothelial wall to maximize their biomechanical effects [14]. However, regular contrast microbubbles are quite small, and in a free flowing situation, the average distance between microbubbles and vessel wall may be too large to produce an optimal effect. Finally, to produce sufficient biomechanical work, microbubbles often need a high US intensity that induces inertial cavitation, with ensuing safety issues.

The concept investigated in the current paper; Acoustic Cluster Therapy (ACT), makes use of similar mechanism as with regular microbubbles, but addresses the shortcomings of the latter. Details and attributes of the ACT formulation concept are described in Ref. [16]. In brief, the approach comprises administration of a dispersion of negatively charged microbubble/positively charged microdroplet clusters, optionally containing a drug payload, followed by a two-step, local US activation and enhancement procedure. US activation induces a liquid-to-gas phase shift of the microdroplet component and the formation of a large bubble that transiently lodge in the microvasculature, occluding blood flow. The subsequent US enhancement step induces controlled volume oscillations that induce enhanced local permeability of the vasculature, allowing extravasation of drug into the tumor tissue extracellular matrix. The concept can hence integrate local drug delivery with enhanced tissue penetration, induced by mild biomechanical effects. Alternatively, the approach can be explored to improve uptake of systemically co-administered drug. The ACT concept represents an unprecedented approach to targeted drug delivery that may improve significantly the efficacy of e.g., current chemotherapy regimen.

In a clinical setting, ACT would represent an image guided, localized therapy; the activated bubble produce copious US backscatter in regular B-mode imaging, giving the operator a tool for confirmation of the spatial distribution and level of bubble deposition. By its nature, ACT would not be indicated towards systemic or strongly metastatic conditions, but towards diseases where it is clinically meaningful to treat known, solid tumors (accessible for US insonation/imaging) with medicinal therapy (e.g., chemotherapy). A number of relevant clinical scenarios exists; most cases where chemotherapy is used as a neo-adjuvant or adjuvant before/after surgical resection, and several diseases where a known, solid and non-resectable tumor is the primary reason for morbidity and mortality. A particularly interesting indication for ACT could be treatment of non-resectable, localized (Stage III) pancreatic ductal adeno-carcinoma (PDAC). These tumors are typically quite easy to image by US. The current standard of care for this condition (gemcitabine in combination with nab-paclitaxel) shows very limited clinical utility and could gain significantly from a combination regime with ACT.

In the current paper, we demonstrate proof of principle for this new treatment strategy, applying US imaging for confirmation of activation and the deposition of large, activated ACT bubbles, and studying delivery and uptake of model drugs, near infrared (NIR) dyes, in a human prostate cancer (PC3) tumor mouse model.

2. Materials and methods

2.1. Mice and tumors

PC-3 prostate adenocarcinoma cells (American Type Culture Collection, USA) were cultured in Dulbecco's modified Eagle medium (Life Technologies, USA) with 10% fetal bovine serum at 37 °C and 5% CO₂. Female Balb/c nude mice (C.Cg/AnNTac-Foxn1 nu NE9, Taconic, Denmark) were purchased at 6–8 weeks of age. The animals were housed in groups of five in individually ventilated cages (IVCs) (Model 1284 L, Techniplast, France). Mice were housed under conditions free of specific pathogens according to the recommendations set by the Federation for Laboratory Animal Science Associations [17]. The mice also had free access to food and sterile water and a controlled environment with temperatures kept between 19 and 22 °C and relative humidity between 50% and 60%. All experimental animal procedures were in compliance with protocols approved by the Norwegian National Animal Research Authorities. Before tumor implantation, mice were anesthetized with isoflurane, and a 50 µl suspension containing 3×10^6 PC-3 cells was slowly injected subcutaneously on the lateral aspect of the left hind leg between the hip and the knee. Tumors were allowed to grow for 4–6 weeks until the diameter of the tumor was between 8 and 10 mm. Anesthesia was induced by subcutaneous (s.c.) injection of midazolam (5 mg/kg)/fentanyl (0.05 mg/kg)/medetomidin (0.5 mg/kg) prior to each intervention as described below. One hour after treatment, an antidote for sedation and anesthesia (atipamezol (2.5 mg/kg) and flumazenil (0.5 mg/kg)) was injected s.c. to wake up the mouse. Mice were kept in a recovery chamber after treatment. Further anesthesia was induced by isoflurane. During all experiments, the mouse body temperature was kept constant.

2.2. Test items

Investigated test items were kindly provided by Phoenix solution, Oslo, Norway. Details are provided in Ref. [16]. In brief, the following formulations were investigated:

- Sonazoid™ (GE Healthcare AS, Norway) [18]; an US contrast agent comprising perfluorobutane (PFB) microbubbles stabilized with a hydrogenated egg phosphatidylserine-sodium (HEPS-Na) phospholipid membrane, embedded in a lyophilized sucrose matrix.
- Non-loaded ACT compound. Microbubble/microdroplet cluster dispersion comprising Sonazoid™ reconstituted with 2 ml of perfluoromethylcyclopentane (PFMCP) microdroplets (3 µl/ml) stabilized with a distearoylphosphatidylcholine (DSCP) phospholipid membrane with 3% (mol/mol) stearylamine (SA), dispersed in 5 mM TRIS buffer.
- Loaded ACT compound. Microbubble/microdroplet cluster dispersion loaded with lipophilic carbocyanine dye 1,1'-dioctadecyl-3,3,3',3'-tetramethylindotricarbocyanine iodide (DiR); Sonazoid™ reconstituted with 2 ml of PFMCP:trichlorofluoropropane: trichloromethane microdroplets (3 µl/ml), containing 10 mg/ml DiR dye, stabilized with a DSCP membrane with 3% (mol/mol) SA, dispersed in 5 mM TRIS buffer.

2.3. Experimental set-up

Characteristics and attributes of ACT were investigated with two techniques; 1) US imaging for elucidation of deposit characteristics and effects on vascularity and 2) optical imaging for demonstration of enhanced uptake and targeted delivery. The experimental set-up is visualized in Fig. 1. In both cases, for activation, the tumor was insonated by regular diagnostic US (DUS) using a clinical VScan system (GE Healthcare AS, Norway), with a transducer (Activation Tx) center frequency of 2.25 MHz and nominal mechanical index (MI) of 0.8 (Peak

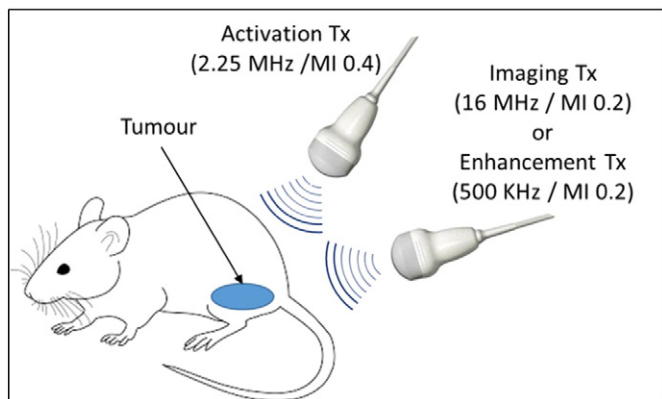


Fig. 1. Illustration of the experimental set-up (Tx = US transducer).

Negative Pressure, PNP, of 1.2 MPa), was used in cardiac mode. Actual MI was measured by a calibrated hydrophone to be approx. 0.40 (PNP of approx. 0.6 MPa) in the insonated tumor volume. For US imaging, a small animal imaging system (Vevo2100, VisualSonics Inc., Canada) with a 16 MHz transducer (Imaging Tx) and a nominal MI of 0.2 (PNP 0.8 MPa) was applied. For optical imaging studies of enhanced uptake and targeted delivery, after activation, the tumor tissue was insonated with low frequency US (LFUS) of 500 kHz at an MI of 0.2 (PNP of 0.14 MPa) using a custom made transducer (Enhancement Tx) (Imasonic SAS, France).

2.4. Ultrasound imaging

2.4.1. In vivo imaging of activation and deposition of ACT bubbles

50 μ l non-loaded ACT compound was injected intravenously (i.v.) and activated by local DUS insonation of tumor tissue for 75 s. ACT contrast enhanced US (CEUS) imaging was performed with the Vevo2100 during the activation procedure and continued post activation in B-mode, linear Contrast imaging mode. The imaging settings were: transmit frequency 16 MHz with a power of 3%. Acquisition: Gain 10 dB, frame rate 10/s. Image display was held constant at a dynamic range of 45 dB, brightness 50, and contrast 50. Activation DUS was turned on at start of injection and 1000 frames were recorded at 10 frames per sec. Time intensity curves (TICs) of the tumor tissues were generated using VisualSonics software. As controls, Sonazoid™ only or microdroplets only, at the same concentration as in the ACT compound, were injected and the same activation and imaging procedures were performed.

2.4.2. Assessment of tumor vasculature

For three animals, before and after activation and deposition of ACT bubbles as described in Section 2.4.1., tumor vasculature was assessed by i.v. injection of 50 μ l Sonazoid™ diluted 1:4 in 5% mannitol solution. The post treatment analysis was performed after complete clearance of the activated bubbles; i.e., >15 min after ACT treatment. CEUS imaging was performed with the Vevo2100 in non-linear contrast mode with a transmit power of 10%, and standard beam width. Image acquisition settings were kept constant for all recording. From the moment of injection of Sonazoid™, 300 frames were recorded at 10 frames per sec. TICs of the tumor tissues were generated using VisualSonics software. Videos pre- and post-ACT treatment were visually compared for market changes in vascularity and vascular patterns. In addition, in order to generate a numeric assessment of global changes in tumor vasculature, TIC curves pre ACT treatment where normalized with TIC curves post treatment. This analysis should detect global changes in in-flow patterns and vascularity through deviations from a horizontal line through 1.

2.5. Quantitative NIR imaging in vivo

A Pearl Impulse Imager (LI-COR Biosciences Ltd., UK) was used for quantitative near infrared fluorescence (NIRF) imaging in vivo. The excitation/emission setting for the 800 nm channel was 785/820 nm. For every data point, a bright light image as well as a NIR image were recorded. Animals were imaged before treatments to establish a background level of fluorescence. The images were analyzed using Pearl Impulse Software (version 2.0). Regions of interest (ROI) for both hind limbs were selected from equivalent-sized areas containing the same number of pixels. ROIs were quantified for total pixel values.

2.5.1. ACT enhanced uptake of co-administered macromolecular infrared (IR) IRDye 800CW-PEG

As a model for a co-injected drug, a vascular contrast agent comprised of an infrared dye attached to a polyethylene glycol (PEG) molecule (IRDye 800CW-PEG; LI-COR) was used [19]. The mice were injected i.v. with 50 μ l of IRDye 800CW-PEG at a final concentration of 5 pmol/g body weight and 50 μ l NaCl or 50 μ l non-loaded ACT compound were injected via tail vein. Activation was performed for 45 s. In one group, the activation step was followed by an enhancement step, insonating the tumor tissue with LFUS, 8 cycle pulses with a pulse repetition frequency of 1 kHz for 5 min.

The animals were imaged directly after treatment (1 min), and after 30 min, 1, 3, 6, and 9 h. 3 groups were compared:

1. Control group (n = 3) received IRDye 800CW-PEG and NaCl, and were then placed on the US treatment rig for 5 min and 45 s before imaging, but received no US.
2. Activation only group (n = 3) received IRDye 800CW-PEG and ACT compound before activation as stated. The mice were then kept in the US treatment rig for an additional 5 min, without applying the low frequency enhancement insonation
3. Activation and enhancement group (n = 5) received IRDye 800CW-PEG and ACT compound before US activation and enhancement steps as stated.

US only groups (i.e. activation US only and enhancement US only) were not included; the applied US procedures, being well below the cavitation threshold, are highly unlikely to induce any bio-effects [20–21] in the absence of gas bodies.

2.5.2. ACT mediated delivery and uptake of lipophilic carbocyanine dye (DiR)

Four mice were injected i.v. with 50 μ l DiR loaded ACT compound via tail vein. As described in Section 2.5.1., DUS and LFUS treatment was applied for 45 s and 5 min, respectively. The animals were imaged directly after treatment and after 30 min. The control group (n = 3) received DiR loaded ACT compound and were transferred to the US treatment set-up for the duration of 5 min and 45 s, but no US was applied.

2.6. Statistical analysis

Results are expressed as mean \pm standard deviation. Statistical comparisons of tumor NIR signal between groups were performed using a two-tailed paired Student's *t*-test. A *p* value less than 0.05 was considered statistically significant.

3. Results and discussion

3.1. In vivo imaging of activation and deposition of ACT bubbles

Upon activation with DUS, appearance and deposition of activated ACT bubbles could be observed as individual, stationary (i.e., non-moving), bright echoes up to 5–10 min after treatment (Fig. 2). Sonazoid™ on the other hand, showed a regular “wash-in/wash-out”

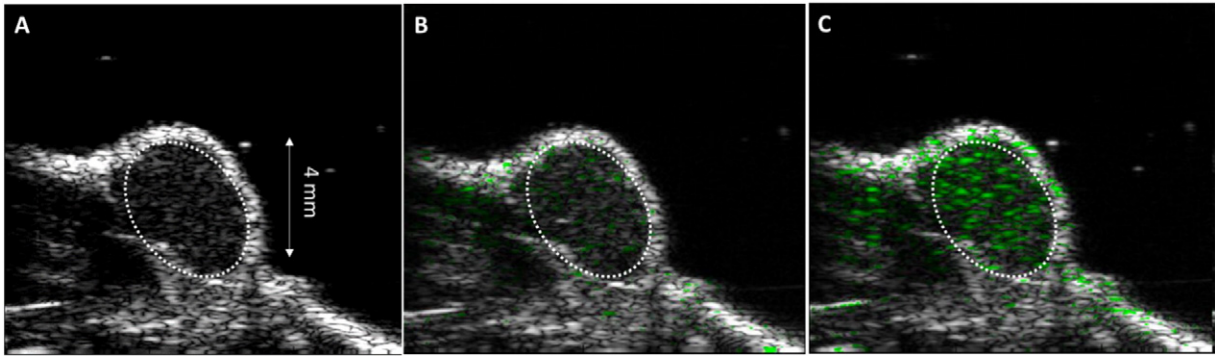


Fig. 2. Vevo2100 images (linear B-mode) of PC3 tumor (marked by dotted line). A) Ultrasound image before treatment (baseline). B) Ultrasound image 90 s after injection of Sonazoid™. C) Ultrasound image 90 s after injection and activation of ACT compound. Large, activated and deposited bubbles are observed as bright, stationary echoes within the tumor volume. Images are color coded to show signal above baseline in green.

pattern with continuously moving echoes, clearing completely after approx. 1 min.

TICs of ACT compound compared to Sonazoid™ and microdroplets control are shown in Fig. 3. Sonazoid showed an initial increase in contrast intensity with a peak (~40 A.U.) after approx. 6 s followed by a rapid decrease back to baseline intensity after approx. 40 s. US activated ACT compound showed an increase to approx. 65 A.U. after approx. 25 s and then remained essentially stable throughout the first 90 s sequence. After approx. 2 min, the contrast signal from the ACT compound started a slow decrease back to baseline after some 15 min. The Sonazoid™ signal was as expected from this US contrast agents [21] and the imaging signal from ACT compound was similar to observations from earlier studies [16]. TICs of the microdroplets only control showed no significant changes of contrast intensity from baseline. This demonstrates, as expected, that DUS does not induce vaporization of the microdroplet component in the absence of an attached microbubble.

Comparing the echo contrast signal from Sonazoid™ to the ACT compound, we clearly identify significant differences in signal characteristics. ACT bubbles appear as stationary, large and bright contrast intensity spots whereas Sonazoid™ as small moving signals, flickering throughout the tumor vasculature. Furthermore, the ACT echoes appear stationary for typically 2–5 min and then dislodge one by one, sometimes intermittently to lodge in a new location, and then to disappear

completely after approx. 15 min. These results confirm the postulated generation and deposit of large activated bubbles upon US insonation of ACT compound.

Qualitative, visual assessment of CEUS images revealed no marked differences in tumor perfusion characteristics, pre- and post-ACT treatment. Comparison of TICs pre- and post-ACT treatment is shown in Fig. 4. As noted, for all animals the ratio of non-linear contrast before and after ACT treatment is close to 1 over the time window investigated demonstrating that ACT does not affect tumor vascular blood flow on a global level in any significant manner. It has earlier been reported that high intensity US in combination with microbubbles can reduce perfusion [22]. Compared to the current study, however, in Ref. [22] significantly higher MI and longer US pulses were applied. The lack of observed vascular effect shows that ACT treatment can be repeated several times in the same tumor.

3.2. ACT enhanced uptake of co-administered macromolecular agent IRDye 800CW-PEG

Typical images from the control (no US) and US activation + enhancement groups are shown in Fig. 5; NIR images showing 800CW-PEG accumulation 1 h after treatment. Notably from these images, no tumor uptake of dye was observed in the control

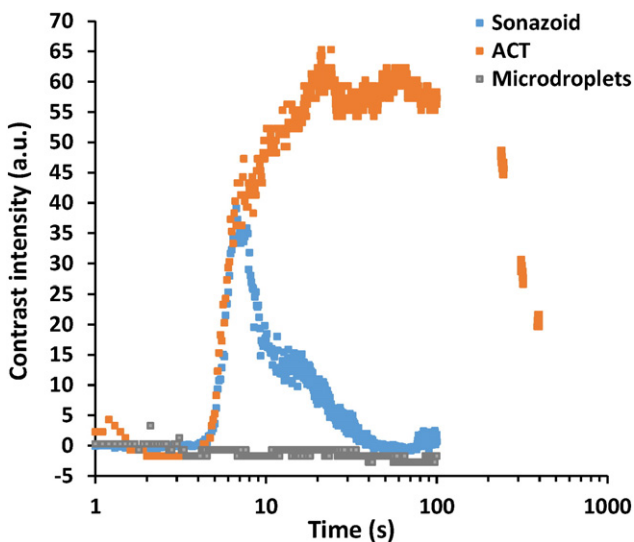


Fig. 3. Time intensity curves (linear B-mode, baseline normalized) of inflow of activated ACT compound (red), Sonazoid™ (blue) and Microdroplets into tumor tissue.

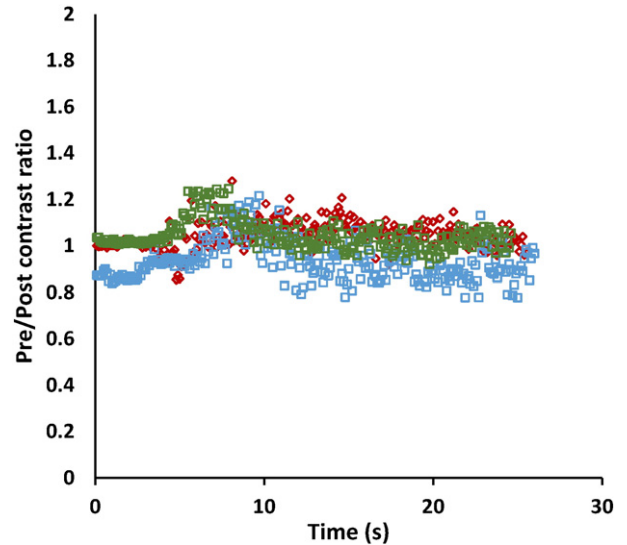


Fig. 4. Time intensity curves (non-linear contrast mode) of inflow of Sonazoid™ pre-ACT treatment, normalized with post-ACT treatment data. Results from three individual animals.

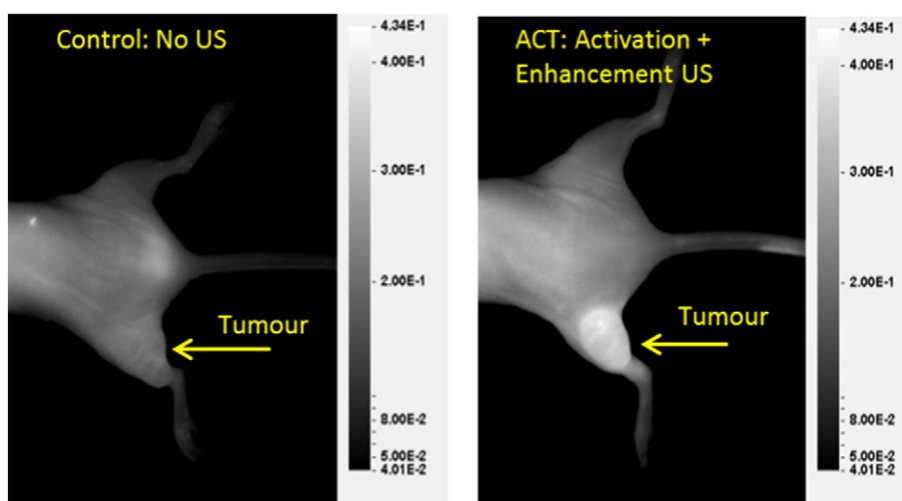


Fig. 5. Typical NIR images of animals receiving 800CW-PEG, with no ACT compound or US treatment (left) and animals receiving 800CW-PEG, ACT compound, and activation and enhancement US treatment (right). Images were taken 1 h after injection.

group, whereas the ACT treated tumor showed clear evidence of a strong uptake, localized to the treated tumor tissue.

For all treatment groups, a NIR signal of $0.15 (\pm 0.02)$ A.U. was observed in the control (right) leg after injection of 800CW-PEG, compared to pre-scan values of auto fluorescence <0.003 A.U. This increase remained constant over 9 h, indicating that amount of 800CW-PEG in the blood vessels plus in the interstitium was constant. No significant differences of the control legs signal intensity between groups was observed.

The uptake of 800CW-PEG in tumors compared to control legs was calculated as tumor to control leg (TCL) ratios in fluorescence intensity (Fig. 6). Compared to auto fluorescence measured at pre-scan, the control group showed no statistically significant increase in NIR signal until 3 h after 800CW-PEG injection. After 3 h, the TCL ratio was $1.38 (\pm 0.07)$, significantly higher than pre-treatment ($p < 0.04$). For the control group the NIR signal continued to increase over time to maximum TCL ratio of $1.5 (\pm 0.05)$ after 9 h. The 800CW-PEG dye is a long circulating, EPR imaging agent and the observed increase in TCL is as expected for this molecule. Directly after treatment, and at every point up to 9 h after treatment, in both groups treated with ACT compound (activation only and activation + enhancement groups), the 800CW-PEG accumulation was significantly higher ($p < 0.01$) compared to control tumors. One minute

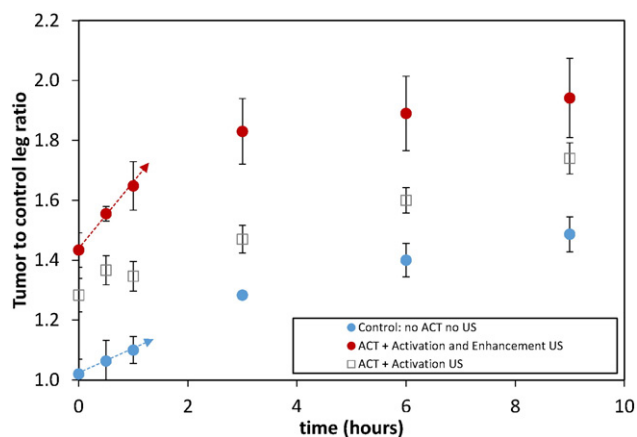


Fig. 6. 800CW-PEG accumulation in tumor tissue. Accumulation is expressed as the ratio of NIR signal between the tumor tissue (left leg) and the contralateral, non-treated leg of the same animal. Error bars are standard error of mean (SEM). Dashed arrows indicate results from linear regression to all data points from 1 min to 1 h within each group (i.e. initial uptake rate).

after treatment, the accumulation increased to TCL values of $1.28 (\pm 0.04)$ and $1.43 (\pm 0.13)$, corresponding to increases of 25% ($p < 0.001$) and 41% ($p < 0.002$) for activation only and activation + enhancement, respectively, compared to the control leg. The maximum difference observed was for the activation + enhancement group, which 1 h after treatment showed a TCL of $1.65 (\pm 0.18)$ compared to $1.10 (\pm 0.04)$ for the control group, an increase of 50% ($p < 0.002$). Linear regressions to all data points from 1 min to 1 h (Fig. 6) showed that the activation + enhancement group displayed more than a doubling in uptake rate for the first hour after treatment compared to the control group; slope of the regression was $0.21 (\pm 0.08) \text{ h}^{-1}$ and $0.08 (\pm 0.08) \text{ h}^{-1}$, for these two groups, respectively. The activation + enhancement group showed statistically higher uptake vs. the activation only group for up to 3 h after treatment, demonstrating that exposing the tumor to the low frequency enhancement US pulse in the presence of the activated ACT compound, increased the delivery of the infrared macromolecular dye.

The observed, instant increase in tumor accumulation of co-injected 800CW-PEG accumulation upon activation of ACT compound shows that transient, local blocking of blood flow can improve penetration of macromolecules in tumors. This might be due to two effects; enhanced vascular permeability caused by the shear forces on the vessel wall increasing the diffusion of molecules across the capillary wall and/or; enhanced transcapillary pressure gradient caused by the blocking bubble increasing the microvascular pressure thereby increasing the convection and fluid flow across the capillary wall [23]. As with other treatments improving convection enhanced delivery [24], this feature of ACT has the potential to enable enhanced delivery of large therapeutic molecules to clinically significant volumes of targeted tissues, offering an improved volume of distribution compared to simple diffusion which is a slow and inefficient process for large molecules [25].

Furthermore, the accumulation of 800CW-PEG was observed to be even higher and more persistent when a low frequency US enhancement step followed the activation step. The oscillations of the large ACT bubbles may also create disruptions in the dense extracellular matrix between tumor cells and/or induce shear forces and streaming thereby improving the tumor tissue distribution of therapeutic molecules even more.

3.3. ACT mediated delivery and uptake of lipophilic carbocyanine dye (DiR)

To study the effect of ACT when the microdroplet contains a payload for local delivery, DiR was used as a model drug. Typical images from the control (no US) and DiR loaded ACT compound + activation and

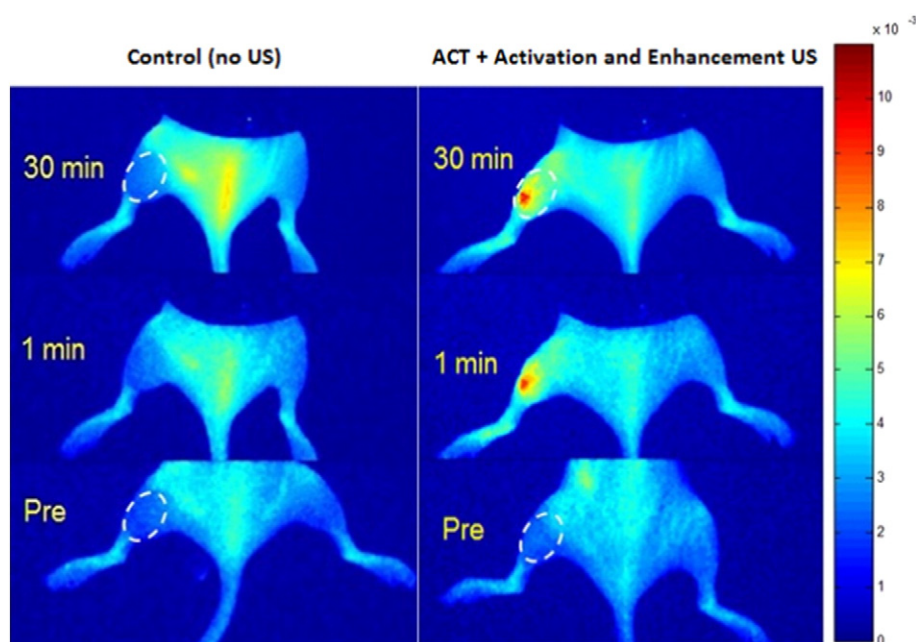


Fig. 7. Local delivery using ACT: near infra-red dye DiR deposition. Tumors ROIs are indicated by dotted line. NIR images before treatment (Pre) and 1 and 30 min after treatment. Left: control (DiR loaded ACT compound, no US treatment). Right: DiR loaded ACT compound + activation and enhancement US insonation.

enhancement US groups are shown in Fig. 7. After administration of DiR loaded ACT compound in the control group, no significant increase in NIR signal was observed in the sham (no US) treated leg during the 30 min of imaging after injection. US treated tumor showed instant DiR delivery, confined to the tumor tissue, with no change over 30 min after treatment. NIR signal intensity, 1 min after treatment, minus pre-treatment signal was on average $2.8 \pm 0.6 \cdot 10^{-3}$ and $0.0 \pm 0.2 \cdot 10^{-3}$, for the treated and control groups respectively. Statistically significant ($p < 0.0008$) delivery and uptake was hence observed for all treated animals.

These results demonstrate the potential of ACT concept to deliver a drug payload locally and specifically to targeted tumor tissue. This speed and extent into solid tumors have not been observed before for a hydrophobic drug [26,27]. From its local release and deposition characteristics, we hypothesize that the ACT concept, and its microscale phase transition attributes, may play a deterministic role in future hydrophobic drug release kinetics.

3.4. Tolerability

The ACT treatment was well tolerated; none of the animals used during the studies sited above showed any sign of discomfort or weight loss after the procedures performed.

4. Conclusions

Developing suitable carriers for targeted drug delivery has proven to be challenging. In the current paper, we provide proof of principle for a relatively simple but versatile drug delivery concept shown to release, hold and enhance tumor uptake of both small hydrophobic molecules loaded into the microbubble and co-injected hydrophilic macromolecules. Increasing the specificity of drug uptake in this manner may significantly reduce the toxicity towards healthy tissue and increase therapeutic efficacy. Studies to show this are under way.

Whereas the mechanisms behind the observed increased and tumor specific uptake are not fully elucidated, it appears that the ACT concept can be applied as a versatile technique for targeted drug delivery, beyond the current delivery paradigm. US controlled local delivery serves a means to deliver therapeutic drugs in an efficient and focused manner

and the ACT concept may allow for local delivery of a wide range of substances such as conventional chemotherapeutic agents, targeted toxins, other proteins, and nanocarriers.

Acknowledgments

The authors thank Siv Eggen, Sigrid Berg, and Kristin Sæterbø for their technical assistance. This work has been partially funded through the Norwegian Research Council grant number 228604.

References

- [1] S.H. Jang, M.G. Wientjes, D. Lu, J.L. Au, Drug delivery and transport to solid tumors, *Pharm. Res.* 20 (2003) 1337–1350.
- [2] K. Greish, Enhanced permeability and retention of macromolecular drugs in solid tumors: a royal gate for targeted anticancer nanomedicines, *J. Drug Target.* 15 (2007) 457–464.
- [3] F. Danhier, O. Feron, V. Preat, To exploit the tumor microenvironment: passive and active tumor targeting of nanocarriers for anti-cancer drug delivery, *J. Control. Release* 148 (2010) 135–146.
- [4] R.K. Jain, T. Stylianopoulos, Delivering nanomedicine to solid tumors, *Nat. Rev. Clin. Oncol.* 7 (2010) 653–664.
- [5] Y.H. Bae, K. Park, Targeted drug delivery to tumors: myths, reality and possibility, *J. Control. Release* 153 (3) (August 10 2011) 198–205.
- [6] Y. Barenholz, Doxil® – the first FDA-approved nano-drug: lessons learned, *J. Control. Release* 160 (2012) 117–134.
- [7] D.A. Yardley, nab-Paclitaxel mechanisms of action and delivery, *J. Control. Release* 170 (2013) 365–372.
- [8] B.P. Timko, T. Dvir, D.S. Kohane, Remotely triggerable drug delivery systems, *Adv. Mater.* 22 (44) (Nov 24 2010) 4925–4943.
- [9] J. Castle, M. Butts, A. Healey, K. Kent, M. Marino, S.B. Feinstein, Ultrasound-mediated targeted drug delivery: recent success and remaining challenges, *Am. J. Physiol. Heart Circ. Physiol.* 304 (2013) H350–H357.
- [10] K.W. Ferrara, Driving delivery vehicles with ultrasound, *Adv. Drug Deliv. Rev.* 60 (10) (Jun 30 2008) 1097–1102.
- [11] I. Lentacker, I. De Cock, R. Deckers, S.C. De Smedt, C.T.W. Moonen, Understanding ultrasound induced sonoporation: definitions and underlying mechanisms, *Adv. Drug Deliv. Rev.* 72 (2014) 49–64.
- [12] S.M. Stiege, C.F. Caskey, R.H. Adamson, S. Qin, F.R. Curry, E.R. Wisner, K.W. Ferrara, Enhancement of vascular permeability with low-frequency contrast-enhanced ultrasound in the chorioallantoic membrane model, *Radiology* 243 (1) (Apr 2007) 112–121.
- [13] K. Kooiman, H.J. Vos, M. Versluis, N. de Jong, Acoustic behavior of microbubbles and implications for drug delivery, *Adv. Drug Deliv. Rev.* 72 (Jun 2014) 28–48.
- [14] H.-L. Liu, C.-H. Fan, C.-Y. Ting, C.-K. Yeh, Combining microbubbles and ultrasound for drug delivery to brain tumors: current progress and overview, *Theranostics* 4 (4) (2014) 432–444.

- [15] B. Geers, H. Dewitte, S.C. De Smedt, I. Lentacker, Crucial factors and emerging concepts in ultrasound-triggered drug delivery, *J. Control. Release* 164 (3) (2012) 248–255.
- [16] P. Sontum, S. Kvåle, A.J. Healey, R. Skurtveit, R. Watanabe, M. Matsumura, J. Østensen, Acoustic cluster therapy (ACT) — a novel concept for ultrasound mediated, targeted drug delivery, *Int. J. Pharm.* 495 (2) (2015) 1019–1027, <http://dx.doi.org/10.1016/j.ijpharm.2015.09.047>.
- [17] W. Nicklas, P. Baneux, R. Boot, T. Decelle, A.A. Deeny, M. Fumanelli, B. Illgen-Wilcke, FELASA, recommendations for the health monitoring of rodent and rabbit colonies in breeding and experimental units, *Lab. Anim.* 36 (1) (Jan 2002) 20–42.
- [18] P.C. Sontum, Physicochemical characteristics of Sonazoid™, a new contrast agent for ultrasound imaging, *Ultrasound Med. Biol.* 34 (5) (2008) 824–833.
- [19] D. Lu, M.G. Wientjes, Z. Lu, J.L. Au, Tumor priming enhances delivery and efficacy of nanomedicines, *J. Pharmacol. Exp. Ther.* 322 (2007) 80–88.
- [20] D.L. Miller, M.A. Averkiou, A.A. Brayman, E.C. Everbach, C.K. Holland, J.H. Wible, J. Wu, Bioeffects considerations for diagnostic ultrasound contrast agents, *J. Ultrasound Med.* 27 (4) (Apr 2008) 611–632.
- [21] T.R. Nelson, J.B. Fowlkes, J.S. Abramowicz, C.C. Church, Ultrasound biosafety considerations for the practicing sonographer and sonologist, *J. Ultrasound Med.* 28 (2) (Feb 2009) 139–150.
- [22] J.M. Correias, L. Bridal, A. Lesavre, A. Mejean, M. Claudon, O. Helenon, Ultrasound contrast agents: properties, principles of action, tolerance, and artifacts, *Eur. Radiol.* 11 (201) 1316–1328.
- [23] D.E. Goertz, M. Todorova, O. Mortazavi, V. Agache, B. Chen, R. Karshafian, K. Hynynen, Antitumor effects of combining docetaxel (taxotere) with the antivascular action of ultrasound stimulated microbubbles, *PLoS One* 7 (2012), e52307.
- [24] L.T. Baxter, R.K. Jain, Transport of fluid and macromolecules in tumors. I. Role of interstitial pressure and convection, *Microvasc. Res.* 37 (1989) 77–104.
- [25] L. Eikenes, M. Tari, I. Tufto, Ø. Bruland, C.d. Davies, Hyaluronidase induces a transcapillary pressure gradient and improves the distribution and uptake of liposomal doxorubicin (Caelyx™) in human osteosarcoma xenografts, *Br. J. Cancer* 93 (2005) 81–88.
- [26] U. Prabhakar, H. Maeda, R.K. Jain, E.M. Sevick-Muraca, W. Zamboni, O.C. Farokhzad, S.T. Barry, A. Gabizon, P. Grodzinski, D.C. Blakey, Challenges and key considerations of the enhanced permeability and retention effect for nanomedicine drug delivery in oncology, *Cancer Res.* 73 (2013) 2412–2417.
- [27] S. Taurin, H. Nehoff, K. Greish, Anticancer nanomedicine and tumor vascular permeability; where is the missing link? *J. Control. Release* 164 (2012) 265–275.